Paper

Organ Dose Reconstruction Applicable for a Japanese Nuclear Worker Cohort: J-EPISODE

Hiroshige Furuta,[1] Kaoru Sato,[2] Akemi Nishide,[3] Shin'ichi Kudo,[1] and Shin Saigusa[1]

Abstract—An evaluation of cancer risk based on organ-absorbed dose is underway for the Japanese Epidemiological Study on Low-Dose Radiation Effects (J-EPISODE), which has analyzed health effects in association with radiation exposure evaluated with the personal dose equivalent $H_p(10)$. Although the concept of effective dose and its operational definition of $H_p(10)$ are widely used for radiological protection purposes, effective dose is not recommended for epidemiological evaluation. Organ-absorbed dose was instead adopted for the IARC 15-Country Collaborative study (15-Country study), the International Nuclear Workers Study (INWORKS), the Mayak worker study, and the Life Span Study (LSS) of atomic bomb survivors. The reconstruction method in J-EPISODE followed in principle the approach adopted in the 15-Country Study. As part of the approach of J-EPISODE, a conversion factor from photon dosimeter reading to air kerma was developed using dosimeter response data, which were measured by the experiment using an anthropomorphic phantom, and it was confirmed that the 15-Country study's assumption of photon energy and geometry distribution in a work environment applied to Japanese nuclear workers. This article focuses on a method for reconstructing the conversion factor from photon dosimeter reading to organ-absorbed photon dose for a Japanese nuclear worker cohort. The model for estimating the conversion factor was defined under the assumption of a lognormal distribution from three concerned bias factors: (1) a dosimeter reading per air kerma, i.e., dosimeter response; (2) an organ-absorbed dose per air kerma; and (3) a factor relating to the differences in dose concepts and calibration practices between the roentgen dosimeter era and the present. Dosimeter response data were cited from the companion paper. Data on organ-absorbed photon dose per air kerma were estimated using a voxel phantom with the average Japanese adult male height and weight. The bias factor for the recorded dose in the roentgen era was defined, considering the backscatter radiation from the human body. The estimated values of organ-absorbed photon dose per air kerma were almost the same as those in ICRP Publication 116, revealing that the effect of differences in body size was almost negligible. The conversion factors from dosimeter reading to organ-absorbed dose were estimated by period (the roentgen era or from then), nuclear facility type (nuclear power plant or other), dosimeter type, and tissue or organ. The estimated conversion factors ranged from 0.7 to 0.9 (Gy Sv^{-1}). The estimated cumulative organ-absorbed photon dose for the participants of J-EPISODE demonstrated that organ-absorbed dose values were approximately 0.8 times the recorded doses if neglecting dose-unit differences. J-EPISODE reconstructed an organ-absorbed dose conversion factor and will evaluate the risk of cancer mortality and morbidity using the organ-absorbed dose in the future.
Health Phys. 121(5):471–483; 2021

Key words: dose, organ; dosimetry, external; epidemiology; nuclear workers

[1]Institute of Radiation Epidemiology, Radiation Effects Association, 1-9-16 Kaji-cho, Chiyoda-ku, Tokyo 101-0044, Japan; [2]Nuclear Science and Engineering Center, Japan Atomic Energy Agency, Tokai-mura, Naka-gun, Ibaraki-ken 319-1195, Japan; [3]Ibaraki Christian University, 6-11-1 Omika, Hitachi, Ibaraki 319-1295, Japan; formerly at Institute of Radiation Epidemiology, Radiation Effects Association.

The authors declare no conflicts of interest.

For correspondence contact: Hiroshige Furuta, Institute of Radiation Epidemiology, Radiation Effects Association, 1-9-16 Kaji-cho, Chiyoda-ku, Tokyo 101-0044, Japan, or email at **furuta@rea.or.jp**.

(*Manuscript accepted* 12 *May* 2021)

0017-9078/21/0

INTRODUCTION

THE NEEDS of organ-absorbed dose

Although the concept of effective dose E and its operational definition of personal dose equivalent $H_p(10)$ are now widely used for radiological protection purposes, the International Commission on Radiological Protection (ICRP) has stated that effective dose is not recommended for epidemiological evaluation (ICRP 2007). It is instead desirable to use organ-absorbed dose for the evaluation of cancer risk in epidemiological cohort studies. Organ-absorbed dose, which is suitably weighted by the relative biological effectiveness (RBE), if necessary, when dealing with neutrons, was adopted for the 15-Country Collaborative Study (hereinafter called the 15-Country study) conducted by the International Agency for Research on Cancer (IARC) (Cardis et al. 2007; Thierry-Chef et al. 2007; Vrijheid et al. 2007). It was also used in the

International Nuclear Workers Study (INWORKS) (Leuraud et al. 2015; Thierry-Chef et al. 2015; Richardson et al. 2015; Hamra et al. 2016), the Mayak worker study (Gilbert et al. 2013), and the Life Span Study (LSS) of atomic bomb survivors, which used RBE-weighted absorbed dose for neutrons (Preston et al. 2007; Ozasa et al. 2012; Grant et al. 2017).

Preceding studies on organ-absorbed dose reconstruction

In the IARC Combined Study, which consisted of seven cohorts in Canada, the United Kingdom, and the United States, Fix et al. (1997) conducted a detailed study of dosimetry technology, radiation fields, and measurement practices, followed by conversion of externally recorded doses to organ-absorbed doses [lung dose and red bone marrow (RBM)]. Thierry-Chef et al. (2007) conducted a study on dose errors within the framework of the 15-Country study and outlined details of the organ-absorbed dose reconstruction method. Thierry-Chef et al. (2015) updated and developed the same method for the INWORKS, which was also an IARC study. Additionally, the Million Worker Study (MWS) also implemented various organ-absorbed dose reconstructions (Bouville et al. 2015). Among these studies, Thierry-Chef et al. (2007) described the method in the most comprehensive and practical detailed manner; therefore, it was used in this study.

Framework for reconstructing the organ-absorbed dose in the 15-Country study

The framework for organ-absorbed dose reconstruction established in the 15-Country study consisted of four main components, as described in Thierry-Chef et al. (2007): (1) experiments of dosimeter response employing readings per $H_p(10)$ for three dosimeter types used until 2000 (the old film badge [FB], a multi-element FB, and a thermoluminescence dosimeter [TLD]); (2) an assumption concerning photon energy and geometry distribution in the workplace; (3) a conversion coefficient from $H_p(10)$ to an organ-absorbed dose derived from ICRP Publication 74 (ICRP 1996); and finally (4) the construction of a conversion factor from dosimeter readings to organ-absorbed dose using the above results in a mathematical model.

Framework for reconstructing the organ-absorbed dose in the J-EPISODE

The Japanese Epidemiological Study on Low-Dose Radiation Effects (J-EPISODE) has been conducted by the Radiation Effects Association (REA) since 1990 and analyzed health effects in association with radiation exposure evaluated with the personal dose equivalent $H_p(10)$ (REA 2015; Kudo et al. 2018a and b). However, among internationally-evaluated radiation epidemiological studies, the organ-absorbed dose has been mainly used for the evaluation of morbidity and mortality due to cancer. For the J-EPISODE

to be compared and evaluated internationally in the future, it is indispensable for it to use an organ-absorbed dose. Additionally, cancer incidence data since 2016 have become available from the National Cancer Registry (Matsuda and Sobue 2015). These conditions have enhanced the J-EPISODE reconstruction of an organ-absorbed dose, and the Expert Committee on Reconstruction of Organ Dose (membership: Michiaki Kai, Norio Tsujimura, Kaoru Sato, and Norihito Sato) was set up within the REA during the fiscal year 2017–2018 (REA 2019). The framework for the conversion from a dosimeter reading to an organ-absorbed dose is displayed in Fig. 1.

The report by the Expert Committee is summarized as follows (REA 2019):

1. The 15-Country study examined the dosimeter response to photon exposure for the dosimeter types FB and TLD. To supplement data for the dosimeter types recently in use, the J-EPISODE experimented on the dosimeter response for radio-photoluminescent glass dosimeters (glass badges [GBs]), active personal dosimeters (hereinafter called electronic personal dosimeter [EPDs]), and optically stimulated luminescence dosimeters (Luminess badges [LBs]) using a device that irradiated an anthropomorphic phantom in the Japan Atomic Energy Agency (JAEA) calibration laboratories, as described by Furuta et al. (2020a). The obtained data were consistent with those in the 15-Country study;

2. The reconstruction of an organ-absorbed dose necessitated information on the photon energy and geometry distribution of the exposed population. The J-EPISODE employed the 15-Country study's assumption concerning photon energy and geometry distribution in a work environment. Simultaneously, to verify the validity of the 15-Country study's assumption in Japan, a literature survey was conducted to review documents on the work environments of Japanese nuclear power plants (NPPs). The literature survey disclosed that Japanese electric power companies had jointly researched energy distribution and incidence direction distribution of gamma rays in the workplace during periodic inspections and maintenance, as well as during plant operation, in the 1980s. The analysis of the survey results on photon energy and geometry distribution at Japanese NPPs demonstrated the appropriateness of applying the 15-Country study's assumption for nuclear workers in Japan and reconstructing an organ-absorbed dose in J-EPISODE, as also described by Furuta et al. (2020b);

3. The 15-Country study applied the conversion factor of an organ-absorbed dose per $H_p(10)$ derived from the conversion coefficient in ICRP Publication 74 (ICRP 1996), which was based on the Reference Computational Phantom-Adult Male (RCP-AM) with standard Caucasian physiques defined in ICRP Publication 110
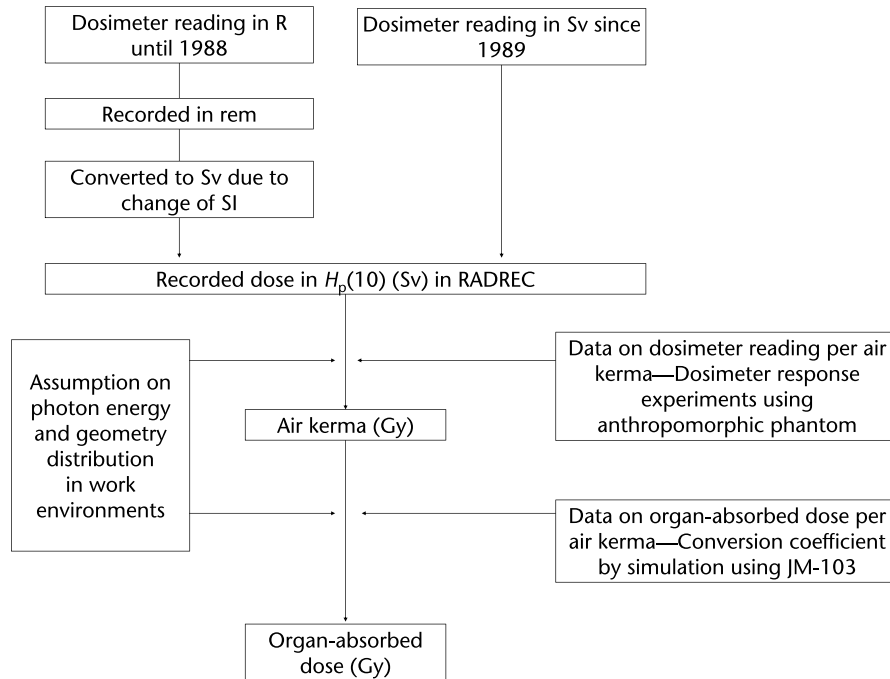
Fig. 1. Framework of reconstruction from dosimeter reading to organ-absorbed dose adopted for the J-EPISODE.

(ICRP 2009). The INWORKS also employed the updated conversion coefficients in ICRP Publication 116 (ICRP 2010). In contrast, the J-EPISODE estimated a conversion coefficient from air kerma to an organ-absorbed dose based on JM-103, an adult male voxel phantom with average Japanese size (Sato et al. 2010, 2011; Sato and Takahashi 2012, 2017; Manabe et al. 2014) that was developed by the JAEA based on ICRP Publication 110 (ICRP 2009); and

4. The above results were integrated using a mathematical model of a lognormal distribution. Finally, the conversion factor from dosimeter reading to organ-absorbed dose was constructed.

Aim of the study

The present study aimed to describe 3. and 4. above and to reconstruct organ-absorbed photon doses from photon dosimeter readings taken from 1957 to 2010 from the J-EPISODE participants. The goal was to reanalyze the data for evaluating radiation risk and confirm the appropriateness of the conversion factors. This manuscript focuses on the conversion from external photon doses only; it briefly addresses other possible sources of radiation exposure for nuclear workers in Japan.

MATERIALS AND METHODS

Study subjects and recorded dose of the J-EPISODE

The J-EPISODE targeted occupationally exposed workers registered with the Radiation Dose Registration

Center (RADREC) (Asano and Ito 2019) within the REA, which included workers in nuclear energy research and development (R&D), nuclear fuel processing, and employed in NPPs, as well as contractors and subcontractors working in NPPs. Each nuclear facility regularly submitted the records of individual annual doses, which were received in the facility and evaluated in $H_p(10)$, to the RADREC. The J-EPISODE was provided with the individual annual doses received in each nuclear facility from 1957 to 2010. This study assumed that the recorded doses were predominantly derived from the photon external exposure with an energy between 100 keV and 3,000 keV.

Model for estimating conversion factors

The model for estimating conversion factors from dosimeter readings to organ-absorbed doses was defined as the following:

$$D_R = T \times B_1 \times B_2 \times B_3, \tag{1}$$

where D_R was the dosimeter reading, T was the organ-absorbed dose, and B_i was the bias factor (i = 1, 2, and 3). B_1 was a reciprocal of the organ-absorbed dose per air kerma, B_2 a dosimeter reading per air kerma, and B_3 a factor relating to the differences in dose concepts and calibration practices. It was considered that T was a true value and that D_R was a measured value including biases. Here, it was assumed that the variables B_1, B_2, and B_3 followed a lognormal distribution for the convenience of calculation:

$$\text{Bias } B_i \sim LN\left(m_i, s_i^2\right), \tag{2}$$

where m_i was the mean of the natural logarithm (ln) of each factor B_i: $\ln(B_i)$, and s_i was the standard deviation of $\ln(B_i)$.

Then, the overall bias B, the products of B_1, B_2, and B_3, also followed a lognormal distribution, as described in the Appendix of the present paper:

$$\text{Overall bias } B \left(= B_1 \times B_2 \times B_3\right) \sim LN\left(m, s^2\right), \tag{3}$$

where m was the sum of the means of $\ln(B_i)$: $m = \Sigma m_i$, and s^2 was the sum of the variances of $\ln(B_i)$: $s^2 = \Sigma s_i^2$.

The bias uncertainty K_i was defined for each bias factor B_i, as follows:

$$K_i = \exp(1.96 \times s_i). \tag{4}$$

Therefore, the 95% confidence interval for the estimated bias B_i was the interval of $(B_i/K_i, B_i \times K_i)$.

The overall uncertainty K of the overall bias B was expressed as the following:

$$K = \exp(1.96 \times s)$$
$$= \exp\left\{ 1.96 \times \text{sqrt}\left[\Sigma \left(\ln K_i / 1.96\right)^2 \right] \right\}. \tag{5}$$

The conversion factor c between the dosimeter reading D_R and the organ-absorbed dose T was expressed as the mean of the overall bias B:

$$c = E(B) = \exp\left(m + s^2/2\right)$$
$$= \exp(m) \times \exp\left(s^2/2\right). \tag{6}$$

The conversion factor c was a constant determined by the period (until 1988 or since 1989), nuclear facility type (NPP or mixed-activities [MA] facility such as R&D organization and fuel processing factory), dosimeter type, and tissue or organ.

The organ-absorbed dose estimated by this method had the following characteristics. The mean value of the estimated organ-absorbed dose (D_R/c) obtained by dividing the recorded dose of each worker by the conversion factor c was equal to the mean value of the true organ-absorbed dose, i.e. an unbiased estimation value. The following equation holds for each year, nuclear facility, and tissue or organ:

$$E(D_R/c) = E(D_R)/c = E(T) \times E(B)/c = E(T). \tag{7}$$

The estimated organ-absorbed dose obtained by dividing the recorded dose for each worker by the conversion factor c should not be interpreted as the organ-absorbed dose for each worker because differences in body size among workers were not taken into consideration. The estimated organ-absorbed dose for a specific worker assumed that the exposure dose followed the same photon energy and geometry distribution as the average of the workers at the nuclear facility and that the body size was the same as the Japanese average.

The uncertainty of the conversion factor c was the same as the overall uncertainty K.

Distribution of photon energy and geometry at the working environment

This study employed the 15-Country study's assumption of photon energy and geometry distribution at workplaces (Thierry-Chef et al. 2007): on average, in NPPs, 10% of the dose received by nuclear workers was due to photon energies ranging from 100 to 300 keV and 90% was from photon energies ranging from 300 to 3,000 keV. In MA facilities, 20% of the dose received by workers was from photon energies ranging from 100 to 300 keV and 80% was from photon energies ranging from 300 to 3,000 keV, with the average geometry being 50% in the antero-posterior (AP) and 50% in the isotropic (ISO) geometry for NPPs and MA facilities. Furuta et al. (2020b) stated that the literature survey results in Japan provided strong evidence that supported the robustness and generality of the 15-Country study's assumption, which was estimated based on the judgments of experts at nuclear facilities around the world.

According to the 15-Country study (Thierry-Chef et al. 2007), the dosimeter response in the 100–300 keV range was considered to be represented by the responses at 118 and 208 keV—the mean energy of beam code N-150 and N-250, respectively—in the experiment. Although this study used responses at 119 and 207 keV, the differences in the mean energy were negligible. Therefore, the dosimeter response in the 100–300 keV range was computed on the weighted average, 25% of which was for the responses at 119 keV and 75% for the responses at 207 keV. In addition, the dosimeter response in the 300–3,000 keV range was considered to be represented by a point at 662 keV. The results representing the energy range of 100–300 keV and 300–3,000 keV were then averaged in the same way for estimating the conversion factor.

B_1 and K_1: Conversion coefficient of an organ-absorbed dose from air kerma for JM-103

The basic data of bias factor B_1 were the reciprocal of the organ-absorbed dose per air kerma by photon energy and geometry. The use of a Japanese adult male phantom was thought appropriate due to the difference in body size from that of a Caucasian male, which was the basis for RCP-AM. The JAEA has developed voxel phantom JM-103 using the average Japanese adult male height and weight (Sato et al. 2010, 2011; Sato and Takahashi 2012, 2017; Manabe et al. 2014), which conformed to the reference voxel phantom RCP-AM defined in ICRP Publication 110 (ICRP 2009). The height and weight of the RCP-AM were 176 cm and 73 kg, respectively, whereas those of the JM-103 were 170 cm and 64 kg.

Concerning the JAEA reports (Sato et al. 2010, 2011; Sato and Takahashi 2012, 2017; Manabe et al. 2014), the ratio of an organ-absorbed dose based on the computational phantoms between RCP-AM and JM-103 by tissue or organ, photon energy (100, 150, 200, 300, 600, and 800 keV), and geometry (AP and ISO) was simulated using the general-purpose radiation transport code PHITS version 2.76, which was developed by the JAEA (Sato et al. 2018). Then, the ratios at energy levels of 119, 207, and 662 keV were interpolated. The selected 14 tissues or organs were the colon, red bone marrow (RBM), esophagus, stomach, liver, gall bladder, spleen, lungs, pancreas, prostate, bladder, kidneys, brain, and heart. Here, the RBM doses for JM-103 and RCP-AM were evaluated by the mass energy absorption coefficient.

The conversion coefficient for JM-103 was estimated by multiplying the above ratio between RCP-AM and JM-103 by the conversion coefficient of organ-absorbed dose per air kerma in ICRP Publication 116 (ICRP 2010) at photon energies of 119, 207, and 662 keV for AP and ISO geometry. Furthermore, the conversion coefficient of an organ-absorbed dose per air kerma under the exposure conditions of NPPs and MA facilities was generated as the weighted mean of the above results, using the proportion values of photon energy and geometry distribution, which was assumed in the 15-Country study (Thierry-Chef et al. 2007).

The uncertainty of the organ-absorbed dose conversion coefficient was considered due to (1) anatomical characteristics (height, organ mass, organ arrangement or shape, etc.), (2) the model used in the simulation code, and (3) statistical errors in the Monte Carlo calculation. However, it was difficult to evaluate the uncertainty quantitatively. In contrast, paragraph 167 of the "Analysis of data variability" in ICRP Publication 74 (ICRP 1996) stated that the coefficients of variation for the calculated organ equivalent dose conversion coefficients were generally less than 2.5% for large organs such as the lungs, liver, and stomach, and less than 1% for organs or tissues distributed throughout the body, such as skin, bone-surface, and bone-marrow. The uncertainty of K_1 was assumed to be 1.050 from $lnK_1 = 1.96 \times 0.025 = 0.049$, since the conversion coefficients were close to 1 and the upper limit of the coefficients of variation was 2.5%.

B_2 and K_2: Dosimeter response

The bias factor B_2 was defined as the dosimeter reading per air kerma by dosimeter type and nuclear facility type. Table 5, "Dosemeter response and uncertainty by dosemeter type and nuclear facility type," in Furuta et al. (2020a) shows bias B_2 and uncertainty K_2 for GB, EPD, and LB, while Figure 6, "Dosimeter response per air kerma in the work environment experienced by nuclear workers by dosimeter type and nuclear facility type," in Furuta et al. (2020a) shows the B_2 for old FB, multi-element FB, and TLD.

Uncertainty K_2 for old FB, multi-element FB, and TLD was determined according to Table 7, "Dosemeter types used in Japan and the corresponding data from the IARC study," in Furuta et al. (2020a), along with the uncertainties in NPPs and MA facilities that were computed as the weighted average of uncertainties derived from the SD/mean in Table 3, "Response of dosemeters irradiated, on phantom, to three radiation qualities (118, 208 and 662 keV) in AP, rotational and isotropic geometries of exposure," in Thierry-Chef et al. (2002).

Table 1. Transition of photon dose concepts and calibration practices in Japan.

Item	Period		
	Until 1988	1989–2000	2001–present
Compliant ICRP Recommendation	Recommendations; Publication 6 (ICRP 1964)	Recommendations; Publication 26 (ICRP 1977)	1990 Recommendations; Publication 60 (ICRP 1991)
Recorded dose by law	Dose equivalent (rem)	Effective dose equivalent (Sv)	Effective dose (Sv)
Operational quantity	–	Personal dose equivalent $H_p(10)$ (Sv)	Same as the left
Physical quantity	Exposure dose (roentgen)	Fluence or air kerma (Gy)	Same as the left
Phantom defining operational quantity	Free air	ICRU sphere phantom (tissue equivalent substance)	ICRU slab phantom (tissue equivalent substance)
Conversion coefficient of operational quantity per physical quantity	–	Dose equivalent per unit fluence at a depth of 10 mm (Table 6 of Publication 51) (ICRP 1987)	$H_p(10)$ per air kerma (Table A24 of Publication 74) (ICRP 1996)
Phantom used for calibration of personal dosimeter in practice	Free air	Acrylic plate phantom	Aquarium water phantom

B_3 and K_3: Bias factor relating to differences in calibration practice and dose concept

The factor B_3 was a specific bias accounting for any differences in dosimeter calibration concepts. Table 1 summarizes the historical changes in the recorded dose quantities and calibration phantoms. Until 1988, the physical quantity of exposure, expressed in terms of its unit the roentgen (R), was measured by personal dosimeters calibrated in free air; therefore, a dosimeter placed on the human body would indicate a reading slightly higher than the delivered exposure due to the backscattered radiation from the body. Thierry-Chef et al. (2007) stated that the backscatter radiation contributed about 10% of the exposure at the surface.

Table 2, "Conversion coefficients between quantities for cesium, cobalt and radium sources," in Thierry-Chef et al. (2007) shows the factors used to convert the recorded dose to $H_p(10)$. The conversion coefficient of $H_p(10)$ per exposure expressed in R was 1.06/100 (Sv R^{-1}) at the calibration source of cesium (662 keV). However, the dosimeter reading expressed in R was directly read as the dose equivalent (rem) in practice because the rem conversion constant per R was set to 1 by regulation (MOL 1975) and was further converted to $H_p(10)$ in Sv using conversion coefficient of 100 rem = 1 Sv due to the change in the International System of Units (SI). Briefly, when 1 R of radiation was directed to a dosimeter placed on the human body, the dosimeter reading indicated 1.1 R. This reading value included backscatter radiation from the body, which read as 1.1 rem and was further recorded as 1.10/100 Sv. The delivered dose of 1 R was evaluated as $H_p(10)$ of 1.06/100 Sv. Therefore, the bias factor B_3 for the recorded doses until 1988 was defined as the ratio between the recorded dose including backscattered radiation expressed in $H_p(10)$ and the delivered dose in $H_p(10)$: $B_3 = (1.10/100) / (1.06/100) = 1/0.96$ (Sv Sv^{-1}).

In contrast, personal dosimeters since 1989 have been designed to measure the phantom-related operational quantities, and therefore any corrections for the specific bias in B_3 were unnecessary. Technically speaking, the period since 1989 can be divided into two periods: (1) 1989–2000 when dosimeters were calibrated on an acrylic slab phantom in terms of $H^*(10)$, as a surrogate for $H_p(10)$, and (2) 2001–present when dosimeters were or are calibrated on a water slab phantom in terms of $H_p(10)$. Compared with the roentgen dosimeter era, however, the transitional changes in calibration conditions appear trivial.

Reconstruction of the organ-absorbed dose from 1957 to 2010

With the use of B_1, B_2, and B_3 above, the conversion factor c (Sv Gy^{-1}) defined in eqn (6) was determined as c (p, ft, dt, t), where p was a period (until 1988 or since 1989), ft was nuclear facility type (NPP or MA facility), dt was dosimeter type (old FB, multi-element FB, TLD,

Table 2. Organ-absorbed dose per air kerma (Gy Gy^{-1}) for JM-103.[a]

Tissue or organ	Antero-posterior geometry Photon energy (keV)			Isotropic geometry Photon energy (keV)			IB_1 (Reciprocal of B_1)		K_1	
	119	207	662	119	207	662	NPP	MA	NPP	MA
Colon	1.38	1.19	1.04	0.70	0.65	0.67	0.84	0.85	1.032	1.029
Red bone marrow (RBM)	1.06	0.92	0.86	0.76	0.68	0.69	0.77	0.78	1.032	1.029
Esophagus	1.11	1.00	0.92	0.64	0.63	0.66	0.78	0.79	1.032	1.029
Stomach	1.48	1.26	1.07	0.71	0.66	0.68	0.86	0.87	1.032	1.029
Liver	1.30	1.13	0.99	0.70	0.65	0.66	0.82	0.82	1.032	1.029
Gall bladder	1.47	1.28	1.09	0.66	0.64	0.66	0.86	0.86	1.032	1.029
Spleen	0.84	0.79	0.78	0.72	0.66	0.67	0.73	0.73	1.032	1.029
Lungs	1.25	1.13	1.03	0.77	0.72	0.74	0.88	0.88	1.032	1.029
Pancreas	1.36	1.18	1.02	0.66	0.59	0.62	0.80	0.81	1.032	1.029
Prostate	1.07	0.98	0.87	0.61	0.58	0.61	0.73	0.74	1.032	1.029
Bladder	1.38	1.18	1.02	0.64	0.61	0.64	0.81	0.82	1.032	1.029
Kidneys	0.92	0.83	0.81	0.66	0.60	0.61	0.70	0.71	1.032	1.029
Brain	0.77	0.76	0.79	0.80	0.77	0.78	0.79	0.79	1.032	1.029
Heart	1.35	1.17	1.02	0.71	0.66	0.69	0.84	0.85	1.032	1.029

[a]Note: (1) RBM was evaluated by the mass energy absorption coefficient. (2) IB_1 was defined as the weighted mean of the above values by energy and geometry using the value of photon energy and geometry distribution. For instance, IB_1 for NPP was computed as:

$IB_{NPP} = \exp[\, 0.025 \times 0.5 \times \ln(IB_{119,\,AP}) + 0.075 \times 0.5 \times \ln(IB_{207,\,AP}) + 0.9 \times 0.5 \times \ln(IB_{662,\,AP}) + 0.025 \times 0.5 \times \ln(IB_{119,\,ISO}) + 0.075 \times 0.5 \times \ln(IB_{207,\,ISO}) + 0.9 \times 0.5 \times \ln(IB_{662,\,ISO}) \,]$. (3) K_1 for NPP was computed using K = 1.05 as the next:

$K_{NPP} = \exp\{1.96 \times \mathrm{sqrt}[\, 0.025 \times 0.5 \times (\ln K/1.96)^2 + 0.075 \times 0.5 \times (\ln K/1.96)^2 + 0.9 \times 0.5 \times (\ln K/1.96)^2 + 0.025 \times 0.5 \times (\ln K/1.96)^2 + 0.075 \times 0.5 \times (\ln K/1.96)^2 + 0.9 \times 0.5 \times (\ln K/1.96)^2 \,]\}$.

GB, EPD, and LB), and t was tissue or organ. The process of reconstructing specific organ-absorbed doses was as follows: (1) the dosimeter type was assigned to the primary personal dosimeter in use at each facility in each year; (2) The annual recorded dose D_R in Sv for each worker exposed at each facility in each year was categorized in relation to the period, nuclear facility type, and dosimeter type was represented as $D_R(w, y, f; p, ft, dt)$, where w was a worker, y was a year between 1957–2010, and f was a facility; and (3) The specific organ-absorbed dose T in Gy for each worker in each year was obtained by dividing the categorized individual annual recorded doses by the corresponding conversion factors and summing them for each worker and year; i.e. $T(w, y, t) = \Sigma_f D_R(w, y, f; p, ft, dt) / c(p, ft, dt, t)$.

Reanalysis of cancer mortality for the J-EPISODE

The excess relative risk (ERR) per Gy for mortality from a specific cancer among the J-EPISODE of a male Japanese nuclear worker cohort was estimated in association with a corresponding organ-absorbed dose using a Poisson

regression model, which was applied to cross-classified data for the number of deaths and person-years. Colon dose, the most representative organ-absorbed dose, was applied for an evaluation of death from all solid cancers, and RBM dose for leukemia. The details of the models have been described elsewhere (REA 2015).

RESULTS

B_1 and K_1: Organ-absorbed dose per air kerma for JM-103

Table 2 summarizes the organ-absorbed dose per air kerma, i.e., organ-absorbed dose conversion factor, by tissue or organ for the Japanese male voxel phantom JM-103 (Sato et al. 2010, 2011; Sato and Takahashi 2012, 2017; Manabe et al. 2014). In the case of AP irradiation in all tissues or organs, the lower the energy, the larger the organ-absorbed dose conversion factor. In contrast, in the case of ISO, the difference due to the energy level was small. The organ-absorbed dose conversion factor for ISO was smaller than that for AP for most tissues or organs and energies. The difference in organ-absorbed dose conversion factors between AP and ISO was small in RBM but large in the colon, stomach, liver, lungs, and other organs.

The organ-absorbed dose conversion factor IB_1, the reciprocal of bias B_1, under the average exposure condition was, for instance, 0.84 (Gy Gy^{-1}) in the colon, 0.88 in the lungs, and 0.77 in RBM for NPPs, and 0.85 in the colon, 0.88 in the lungs, and 0.78 in RBM for MA facilities. The values of IB_1 for the lungs and colon, which are located in the anterior surface part of the body, were larger than that of RBM, which is situated deep in the body.

B_2 and K_2: Dosimeter reading per air kerma

Table 3 shows the dosimeter response B_2, i.e., dosimeter reading per air kerma and its uncertainty K_2 by dosimeter

Table 3. Dosimeter response and uncertainty by dosimeter type and nuclear facility type.[a]

Dosimeter type	Dosimeter Response (B_2) (Sv Gy^{-1})		Uncertainty (K_2)	
	NPP	MA	NPP	MA
Old FB	1.07	1.10	1.034	1.063
Multi-element FB	1.06	1.07	1.026	1.051
TLD	1.02	1.04	1.034	1.048
GB	1.02	1.02	1.011	1.011
EPD	1.00	1.01	1.004	1.003
LB	1.06	1.08	1.037	1.033

[a]Note: (1) Dosimeter response B_2 and uncertainty K_2 for GB, EPD, and LB cited Table 5 of Furuta et al. (2020a). (2) Dosimeter response B_2 for old FB, multi-element FB, and TLD refers to Figure 6 in Furuta et al. (2020a). (3) Uncertainty K_2 for old FB, multi-element FB, and TLD were determined according to Table 7 of Furuta et al. (2020a), along with the uncertainties in NPP or MA that were computed as the weighted average of uncertainties derived from the SD/mean in Table 3 of Thierry-Chef et al. (2002).

Table 4. Bias for the recorded dose until 1988 and its uncertainty.

Period	Quantity	B_3	K_3
Until 1988	Exposure in R[a]	1/0.96 (Sv Sv^{-1})	1.103 (s = 0.05)
Since 1989	$H_p(10)$	1	1 (s = 0)

[a]Despite the relationship of one rem being equivalent to 0.96 R, the value of dosimeter reading in R were in practice recorded in rem as it was until 1988, then converted to Sv due to the change of SI in 1989.

type and nuclear facility type. The values of dosimeter responses were between 1.0–1.1 (Sv Gy^{-1}). The dosimeter responses for MA facilities were about 2% larger than those for NPPs. By dosimeter type, the dosimeter responses for FB and LB were relatively large, while those for EPD, GB, and TLD were close to 1.

B_3 and K_3: Bias factor for the recorded dose until 1988

Table 4 shows the bias factor B_3 related to calibration practice and dose concept as well as its uncertainty K_3. For the recorded doses in Sv until 1988, which were derived from reading the exposure in R, bias factor B_3 was 1/0.96 (Sv Sv^{-1}) and its uncertainty K_3 was 1.103. For the recorded dose since 1989, B_3 and K_3 were set to 1 for convenience.

Conversion factor from dosimeter reading to organ-absorbed dose

Table 5 shows the values of the first term of exp(m) in eqn (6) by period, dosimeter type, and nuclear facility type for the colon, lungs, and RBM, as well as the associated

Table 5. The first term of eqn (6) of the conversion factor c by period, nuclear facility type, and dosimeter type for the colon, lungs, and RBM, as well as its uncertainty.[a]

Dosimeter type	NPPs			MA facilities			Overall uncertainty K	
	Colon	Lungs	RBM	Colon	Lungs	RBM	NPP	MA
exp(m): the first term of eqn (6) since 1989								
Multi-element FB	1.26	1.20	1.38	1.26	1.22	1.37	1.041	1.059
TLD	1.21	1.16	1.32	1.22	1.18	1.33	1.047	1.056
GB	1.21	1.16	1.32	1.20	1.16	1.31	1.034	1.031
EPD	1.19	1.14	1.30	1.19	1.15	1.29	1.032	1.029
LB	1.26	1.20	1.38	1.27	1.23	1.38	1.049	1.044
exp(m): the first term of eqn (6) until 1988								
Old-FB	1.33	1.27	1.45	1.35	1.30	1.47	1.114	1.126
Multi-element FB	1.31	1.25	1.43	1.31	1.27	1.43	1.112	1.120
TLD	1.26	1.21	1.38	1.27	1.23	1.39	1.114	1.119

[a]Note: (1) The first term of eqn (6) was computed as follows:

exp(m) = $B_1 \times B_2 \times B_3$ = (1/IB_1) $\times$ $B_2 \times B_3$. (2) By each period, only the dosimeter types used in that period were displayed. (3) Overall uncertainty K was computed using eqn (5).

Table 6. The second term of eqn (6) of the conversion factor c by period, nuclear facility type, and dosimeter type for the colon, lungs, and RBM.[a]

Dosimeter type	NPPs			MA facilities		
	Colon	Lungs	RBM	Colon	Lungs	RBM
$\exp(s^2/2)$: the second term of eqn (6) since 1989						
Multi-element FB	1.0004	1.0004	1.0004	1.0004	1.0004	1.0004
TLD	1.0004	1.0004	1.0004	1.0004	1.0004	1.0004
GB	1.0001	1.0001	1.0001	1.0001	1.0001	1.0001
EPD	1.0001	1.0001	1.0001	1.0001	1.0001	1.0001
LB	1.0003	1.0003	1.0003	1.0002	1.0002	1.0002
$\exp(s^2/2)$: the second term of eqn (6) until 1988						
Old-FB	1.002	1.002	1.002	1.002	1.002	1.002
Multi-element FB	1.002	1.002	1.002	1.002	1.002	1.002
TLD	1.002	1.002	1.002	1.002	1.002	1.002

[a]Note: The values of $\exp(s^2/2)$, the second term of eqn (6) were computed as:
$\exp(s^2/2) = \exp\{ [(\ln K_1/1.96)^2 + (\ln K_2/1.96)^2 + (\ln K_3/1.96)^2]/2 \}$.

overall uncertainty K. The values of the second term of exp $(s^2/2)$ in eqn (6), which had a role in contributing the uncertainty of bias to the conversion factor, are shown in Table 6. The values of the second term were negligible, both until 1988 (1.002 for all) and since 1989 (1.0001–1.0004). Therefore, the values of the conversion factor were basically determined by the values of the first term. Table 7 shows the reciprocal of the conversion factor (1/c) by period, nuclear facility type, and dosimeter type for the colon, lungs, and RBM.

The values of the reciprocal of conversion factors were from approximately 0.7 (Gy Sv^{-1}) to 0.9. Fig. 2 shows the reciprocal of conversion factor for EPD at NPPs since 1989 by tissue or organ in order of values. The values were higher in the lungs (0.88), stomach (0.86), and gall bladder (0.86), whereas they were lower in the kidneys (0.70), prostate (0.73), and spleen (0.73).

DISCUSSION

Differences in the 15-Country study and the INWORKS organ-absorbed dose reconstruction methods

This study followed in principle the 15-Country study's organ-absorbed dose reconstruction method described by Thierry-Chef et al. (2007). This method was also used in the INWORKS, as described by Thierry-Chef et al. (2015). Although the INWORKS updated the dosimeter response data, changed the organ-absorbed dose conversion factor from ICRP Publication 74 (ICRP 1996) to Publication 116 (ICRP 2010), and created a time-varying variable to address the neutron exposure condition, the basic framework for converting photon dosimeter readings to organ-absorbed photon doses remained unchanged, even after Thierry-Chef et al. (2015).

Differences in the 15-Country study and the INWORKS facility development times and cohort compositions

Since the 15-Country study and the INWORKS included some facilities that began to operate before the 1950s, much effort was devoted to the comparability of dose concepts and dosimeter calibration practices. In contrast, the Japanese nuclear industry started in the late 1950s; consequently, the concept of exposure dose in R was used from the outset (Table 1). This late start contributed to the simplification of factor B_3 compared with the IARC studies.

Most Japanese nuclear workers worked at NPPs, where half of the reactors were pressurized water reactors (PWRs) and half were boiling water reactors (BWRs). The main source of the photon dose was ^{60}Co. There were no measurable records of neutron exposure from the operating reactor exceeding the detection limit. Moreover, there was no internal exposure to tritium because there was no heavy water reactor (HWR) in Japan.

Additionally, the 15-Country study and the INWORKS included nuclear weapons manufacturing operations in the 1940s and 1950s. Consequently, neutron exposure was a major issue. This study did not encounter this issue because the manufacturing of nuclear weapons has been banned since 1955 under the Japan-US agreement concerning civil uses of atomic energy and related domestic acts in Japan.

Sources of radiation exposure and uncertainties for the J-EPISODE

The organ-absorbed dose reconstruction method described in this study dealt with photon doses only. Fix et al. (1997) and Merwin et al. (2008) discussed in detail the sources of radiation and the possible causes of errors in dosimetry for the IARC Combined Study and Part B of the Energy Employees Compensation Act, respectively. The actions taken in Japan to address these potential problems can

Table 7. Conversion factor from dosimeter reading to organ-absorbed dose by period, nuclear facility type, and dosimeter type for the colon, lungs, and RBM.[a]

Dosimeter type	NPPs			MA facilities		
	Colon	Lungs	RBM	Colon	Lungs	RBM
1/c: reciprocal of conversion factor (Gy Sv^{-1}) since 1989						
Multi-element FB	0.79	0.83	0.73	0.79	0.82	0.73
TLD	0.82	0.86	0.75	0.82	0.85	0.75
GB	0.82	0.86	0.75	0.83	0.86	0.76
EPD	0.84	0.88	0.77	0.84	0.87	0.77
LB	0.79	0.83	0.73	0.79	0.81	0.72
1/c: reciprocal of conversion factor (Gy Sv^{-1}) until 1988						
Old FB	0.75	0.79	0.69	0.74	0.77	0.68
Multi-element FB	0.76	0.80	0.70	0.76	0.79	0.70
TLD	0.79	0.83	0.72	0.78	0.81	0.72

[a]Note: (1) The value c was computed as the product of Tables 5 and 6. (2) The organ-absorbed dose is obtained by multiplying the recorded dose in Sv by (1/c), the reciprocal of the conversion factor.
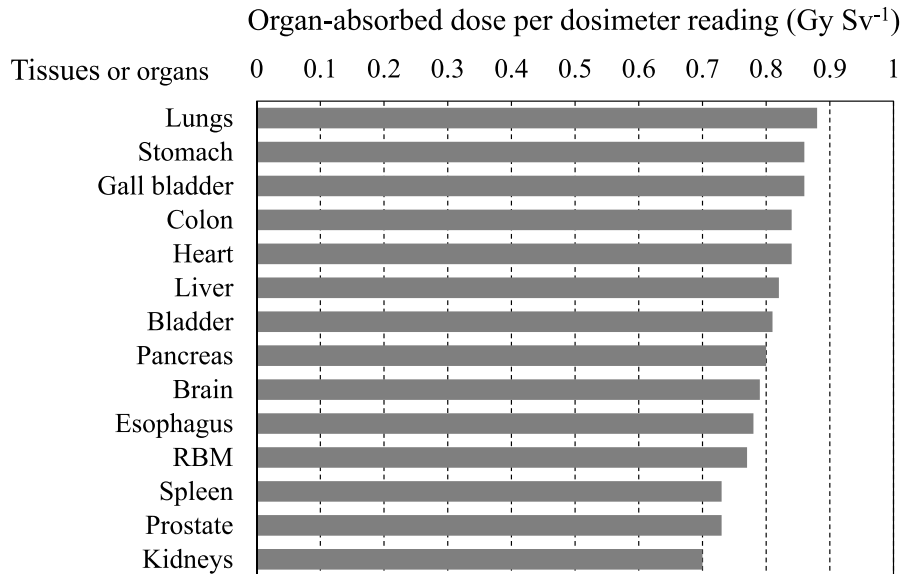
Organ-absorbed dose per dosimeter reading (Gy Sv^{-1})

Fig. 2. Conversion factors from dosimeter reading to organ-absorbed dose for the selected 14 tissues or organs (EPD at NPPs since 1989).

be summarized as follows: (1) a medical examination, including a chest x ray, is implemented annually by law, but exposure dose unrecorded; (2) workers are not allowed to enter the controlled area without wearing a personal dosimeter; (3) film badges are to be changed monthly; (4) doses below the detection limit are never recorded as zero, and the RADREC database instead records the number of entries into the controlled area that are below the detection limit; and (5) to address the storage dose for the integrating personal dosimeter, a control dosimeter is to be used to exclude the effect of background radiation.

The study covered the exposure dose resulting from normal work—the work during the operation, periodic inspection, and maintenance in case of NPP—from 1957 to 2010. During the period, neutron exposure was limited only for a few workers, and internal emitter was rare; therefore, the organ-absorbed dose reconstruction and the risk analysis proceeded under the assumption that the recorded dose was predominantly due to photon radiation. In practice, original records of neutron exposure doses and internal doses evaluated in committed doses, if any, are to be kept by each employer. In contrast, by regulation, this information is not recorded in the RADREC database, which includes only the individual annual dose (external dose plus internal dose). After lifting the designation of a nuclear worker, his disaggregated records into external and internal doses are to be sent to the RADREC. However, there is no breakdown of neutron exposure in this document either. Despite thorough investigation and discussion, it is not feasible to identify workers with possible neutron exposure, meaning that it does not make much sense to pursue breakdown into neutron.

During the fabrication of mixed oxide (MOX) fuel containing 20–30% plutonium by weight for the experimental

fast breeder reactor Joyo and the prototype reactor Monju at the Nuclear Fuel Cycle Engineering Laboratories (NCL) of JAEA for a certain period, at most 200–300 workers were possibly exposed to neutrons and photons, specifically 60 keV photons from [241]Am. However, even for those workers, the contribution of neutron to the effective dose was only about 30% (Yamazaki et al. 2017; Tsujimura et al. 2021). The JAEA-NCL's neutron exposure has existed since the 1980s and has used albedo-type TLD dosimeters. Because the JAEA-NCL has not used a neutron track emulsion type A (NTA) film dosimeter, which has been mentioned by Merwin et al. (2008) and Thierry-Chef et al. (2015) as having a technical defect in that neutrons of about 0.5 MeV or less could not be measured, such problems have not historically occurred in the JAEA.

There have been some cases of internal exposure, but most of them have been minor until 2010. For instance, from the experience of plutonium inhalation accidents in the past decades at the JAEA-NCL, the exposure of one worker in 1993 with an effective dose equivalent of 90 mSv was the largest by far, and the others were trivial, being an average of 0.1 mSv at the MOX plant and 1.5 mSv at the reprocessing plant (Kurihara and Kanai 2011).

After 2010, there were cases of an accident at the TEPCO Fukushima Daiichi Nuclear Power Plant (FDNP) in March 2011, as well as a plutonium contamination accident at the Oarai R&D Institute of JAEA in June 2017 where five workers were internally exposed. In the FDNP accident, there was an internal exposure to ^{131}I and other radionuclides, but the evaluation of internal dose due to emergency work and conversion to an annual organ-absorbed dose is ongoing.

Thus, neutron exposure doses and internal exposure doses, if any, were ignored in organ-absorbed dose reconstruction in the present study.

Differences in body size between Caucasians and Japanese

Regarding the estimation of the organ-absorbed dose per air kerma, the standard Caucasian male phantom RCP-AM was used in the 15-Country study, whereas the average Japanese adult male phantom JM-103 was used in this study. The value of an organ-absorbed dose in the colon and lungs based on JM-103 was about 2% larger than its RCP-AM value (Table 8). Because the Japanese are smaller in body size than Caucasians, their subcutaneous tissue in the abdomen and chest is accordingly thinner. Regarding RBM, in which hematopoietic function is distributed in many tissues, no difference was observed between the two phantoms. At least for adult males, the effect of differences in body size was almost negligible.

Regarding the values of dosimeter response, Furuta et al. (2020a) stated that the results for GB, EPD, and LB in their study were compatible with the results of FB and TLD in the 15-Country study. Therefore, the results of the conversion factor of the present study apply to nuclear worker cohort studies in other countries.

Recently, mesh phantoms have been developed. The voxel phantom can be expressed in mm, whereas the mesh phantom can be described in μm, which allows, for example, an evaluation of the bone surface. However, for the tissues or organs concerned in the present study, mesh phantoms are unlikely to affect the results.

Robustness and generality of the 15-Country study's assumption

Table 2 demonstrates the differences in the values of organ-absorbed dose per air kerma between the AP and ISO for all tissues or organs. This result indicated that the geometry distribution was a strong contributor in estimating the weighted mean for the work environments of NPPs or MA facilities. In such a context, it was crucial that the 15-Country study's assumption of photon energy and geometry distribution was supported by the literature survey results in Japan, as mentioned by Furuta et al. (2020b), indicating the robustness and generality of the assumption.

Reconstruction of the organ-absorbed dose from 1957 to 2010

Table 9 shows the comparison of the cumulative dose between the recorded dose in $H_p(10)$ and a specific organ-absorbed dose reconstructed for the J-EPISODE. While the mean cumulative dose in $H_p(10)$ was 13.9 mSv in 2010,

Table 8. Comparison of organ-absorbed dose per air kerma between RCP-AM and JM-103 for the colon, lungs, and RBM (Gy Gy^{-1}).

Phantom	NPPs			MA facilities		
	Colon	Lungs	RBM	Colon	Lungs	RBM
RCP-AM	0.82	0.86	0.77	0.83	0.87	0.78
JM-103	0.84	0.88	0.77	0.85	0.88	0.78

Table 9. Comparison of cumulative dose between $H_p(10)$ and a specific organ-absorbed dose (1957–2010 for 204,103 male workers in the J-EPISODE).

	Recorded dose $H_p(10)$ (mSv)	Organ-absorbed dose (mGy)		
		Colon	Lungs	RBM
Mean cumulative dose in 2010	13.9	11.0	11.5	10.1

the mean cumulative organ-absorbed dose was 11.0 mGy for the colon, 11.5 mGy for the lungs, and 10.1 mGy for RBM. Neglecting dose-unit differences, organ-absorbed dose values were approximately 0.8 times the recorded doses.

This difference of 0.8 between the measured doses and the organ-absorbed doses was fundamentally derived from the estimates of dosimeter responses, the organ-absorbed dose conversion factors used, and the assumption of photon energy distribution and geometry distribution. Of these, the first two were technically determined, so they were thought to be common in all studies. However, the differences in the exposure scenarios of geometry distribution have an impact. The present study, along with the 15-Country study and the INWORKS, assumed that 50% of the exposure dose was in AP and 50% in ISO. In contrast, 50% in AP and 50% in rotational (ROT) geometry was adopted in the IARC Combined Study (Fix et al. 1997). In addition, the MWS recommended using 70% in AP and 30% in ROT if detailed information was not available (Bouville et al. 2015).

As for the results of the INWORKS, the reciprocal of the estimated bias, B_{colon}, B_{lung}, and B_{RBM} for men in Table 1 of Thierry-Chef et al. (2015), corresponded to the ratio of the measured dose to the organ-absorbed dose. The results of the present study were compatible with this finding.

Reanalysis of cancer mortality for the J-EPISODE

For all 204,103 participants in the cohort during the follow-up period 1991–2010, the ERRs Gy^{-1} were estimated for several cancers in association with organ-absorbed doses. Reanalysis results of cancer mortality for the J-EPISODE will be presented separately. Ignoring dose units, the values of the ERRs Gy^{-1} were slightly larger than, or rather about the same as, the corresponding values of the ERRs Sv^{-1} in the previous analysis using $H_p(10)$ (REA 2015), indicating the appropriateness of using the conversion factor from dosimeter readings to organ-absorbed doses for further analysis.

CONCLUSION

The J-EPISODE constructed an organ-absorbed dose conversion factor. Accordingly, the J-EPISODE will use the organ-absorbed dose to estimate the risk of cancer mortality and cancer incidence in the future. A series of companion papers to the present study demonstrated that the 15-Country study's assumption of photon energy and geometry distribution

was robust and general. The dosimeter response data for GB, EPD, and LB were consistent with the 15-Country study and will also be useful for any nuclear worker cohorts. The differences in radiation effects on tissues or organs between the Caucasian and Japanese models were small. Therefore, the conversion factors from dosimeter reading to organ-absorbed dose revealed in the present study can be applied to nuclear worker cohort studies in other countries.

REFERENCES

Asano T, Ito A. Experience and perspective on radiation dose registry in Japan. Jpn J Health Phys 54:135–136; 2019.

Bouville A, Toohey RE, Boice JD Jr, Beck HL, Dauer LT, Eckerman KF, Hagemeyer D, Leggett RW, Mumma MT, Napier B, Pryor KH, Rosenstein M, Schauer DA, Sherbini S, Stram DO, Thompson JL, Till JE, Yoder C, Zeitlin C. Dose reconstruction for the million worker study: status and guidelines. Health Phys 108:206–220; 2015.

Cardis E, Vrijheid M, Blettner M, Gilbert E, Hakama M, Hill C, Howe G, Kaldor J, Muirhead CR, Schubauer-Berigan M, Yoshimura T, Bermann F, Cowper G, Fix JJ, Hacker C, Heinmiller B, Marshall M, Thierry-Chef I, Utterback D, Ahn Y-O, Amoros E, Ashmore P, Auvinen A, Bae J-M, Bernar J, Biau A, Combalot E, Deboodt P, Diez Sacristan A, Eklof M, Engels H, Engholm G, Gulis G, Habib RR, Holan K, Hyvonen H, Kerekes A, Kurtinaitis J, Malker H, Martuzzi M, Mastauskas A, Monnet A, Moser M, Pearce MS, Richardson DB, Rodriguez-Artalejo F, Rogel A, Tardy H, Telle-Lamberton M, Turai I, Usel M, Veress K. The 15-country collaborative study of cancer risk among radiation workers in the nuclear industry: estimates of radiation-related cancer risks. Radiat Res 167:396–416; 2007.

Fix JJ, Salmon L, Cowper G, Cardis E. A retrospective evaluation of the dosimetry employed in an international combined epidemiological study. Radiat Protect Dosim 74:39–53; 1997.

Furuta H, Tsujimura N, Nishide A, Kudo S, Saigusa S. Conversion factor from dosemeter reading to air kerma for nuclear worker using anthropomorphic phantom for further conversion from air kerma to organ-absorbed dose. Radiat Protect Dosim 189:371–383; 2020a.

Furuta H, Nishide A, Kudo S, Saigusa S. Estimation of photon energy and direction distributions at Japanese nuclear power plants based on literature survey for J-EPISODE study. Radiat Protect Dosim 190:372–391; 2020b.

Gilbert ES, Sokolnikov ME, Preston DL, Schonfeld SJ, Schadilov AE, Vasilenko EK, Koshurnikova NA. Lung cancer risks from plutonium: an updated analysis of data from the Mayak worker cohort. Radiat Res 179:332–342; 2013.

Grant EJ, Brenner A, Sugiyama H, Sakata R, Sadakane A, Utada M, Cahoon EK, Milder CM, Soda M, Cullings HM, Preston DL, Mabuchi K, Ozasa K. Solid cancer incidence among the Life Span Study of atomic bomb survivors: 1958–2009. Radiat Res 187:513–537; 2017.

Hamra GB, Richardson DB, Cardis E, Daniels RD, Gillies M, O'Hagan JA, Haylock R, Laurier D, Leuraud K, Moissonnier M, Schubauer-Berigan M, Thierry-Chef I, Kesminiene A. Cohort profile: the international nuclear workers study (INWORKS). Int J Epidemiol 45:693–699; 2016.

International Commission on Radiological Protection. Recommendations of the International Commission on Radiological Protection. Oxford: Pergamon Press; ICRP Publication 6; 1964.

International Commission on Radiological Protection. Recommendations of the International Commission on Radiological Protection. Oxford: Pergamon Press; ICRP Publication 26; Ann. ICRP 1(3); 1977.

International Commission on Radiological Protection. Data for use in protection against external radiation. Oxford: Pergamon Press; ICRP Publication 51; Ann. ICRP 17(2/3); 1987.

International Commission on Radiological Protection. 1990 recommendations of the International Commission on Radiological Protection. Oxford: Pergamon Press; ICRP Publication 60; Ann. ICRP 21(1/3); 1991.

International Commission on Radiological Protection. Conversion coefficients for use in radiological protection against external radiation. Oxford: Pergamon Press; ICRP Publication 74; Ann. ICRP 26(3/4); 1996.

International Commission on Radiological Protection. The 2007 recommendations of the International Commission on Radiological Protection. Oxford: Pergamon Press; ICRP Publication 103; Ann. ICRP 37(2/4); 2007.

International Commission on Radiological Protection. Adult reference computational phantoms. Oxford: Pergamon Press; ICRP Publication 110; Ann. ICRP 39(2); 2009.

International Commission of Radiological Protection. Conversion coefficients for radiological protection quantities for external radiation exposures. Oxford: Pergamon Press; ICRP Publication 116; Ann. ICRP 40(2/5); 2010.

Kudo S, Ishida J, Yoshimoto K, Mizuno S, Ohshima S, Furuta H, Kasagi F. Direct adjustment for confounding by smoking reduces radiation-related cancer risk estimates of mortality among male nuclear workers in Japan, 1999–2010. J Radiol Prot 38:357–371; 2018a.

Kudo S, Yoshimoto K, Furuta H, Inoue K, Fukushi M, Kasagi F. Occupational radiation exposure and leukemia mortality among nuclear workers in Japan: J-EPISODE, 1991–2010. Jpn J Health Phys 53:146–153; 2018b.

Kurihara O, Kanai K. Individual monitoring for internal contamination with plutonium compounds at JAEA-NCL. Radiat Protect Dosim 146:144–147; 2011.

Leuraud K, Richardson DB, Cardis E, Daniels RD, Gillies M, O'Hagan JA, Hamra GB, Haylock R, Laurier D, Moissonnier M, Schubauer-Berigan MK, Thierry-Chef I, Kesminiene A. Ionizing radiation and risk of death from leukaemia and lymphoma in radiation-monitored workers INWORKS: an international cohort study. Lancet Haematol 2:e276–e281; 2015.

Manabe K, Sato K, Endo A. Comparison of internal doses calculated using the specific absorbed fractions of the average adult Japanese male phantom with those of the reference computational phantom-adult male of ICRP publication 110. Phys Med Biol 59:1255–1270; 2014.

Matsuda T, Sobue T. Recent trends in population-based cancer registries in Japan: the act on promotion of cancer registries and drastic changes in the historical registry. Int J Clin Oncol 20:11–20; 2015.

Merwin SE, Smith MH, Winslow RC, McCartney KA, Fix JJ, Taulbee TD, Macievic GL. External dose reconstruction under part B of the energy employees compensation act. Health Phys 95:95–106; 2008.

Ministry of Labor. Guide to prevent ionizing radiation hazards. Tokyo: Japan Industrial Safety and Health Association; 1975 (in Japanese).

Ozasa K, Shimizu Y, Suyama A, Kasagi F, Soda M, Grant EJ, Sakata R, Sugiyama H, Kodama K. Studies of the mortality of atomic bomb survivors: Report 14, 1950–2003: an overview of cancer and noncancer diseases. Radiat Res 177:229–243; 2012.

Preston DL, Ron E, Tokuoka S, Funamoto S, Nishi N, Soda M, Mabuchi K, Kodama K. Solid cancer incidence in atomic bomb survivors: 1958–1998. Radiat Res 168:1–64; 2007.

Radiation Effects Association. Summary of the fifth study report on low-dose radiation effects on human health [online]. 2015. Available at ***http://www.rea.or.jp/ire/pdf/Summary_Fifth_Study_Report.pdf***. Accessed 10 May 2021.

Radiation Effects Association. Report of the expert committee on organ dose reconstruction [online]. 2019 (in Japanese but abstract available in English). Available at ***http://www.rea.or.jp/ire/pdf/zouki.pdf***. Accessed 10 May 2021.

Richardson DB, Cardis E, Daniels RD, Gillies M, O'Hagan JA, Hamra GB, Haylock R, Laurier D, Leuraud K, Moissonnier M, Schubauer-Berigan MK, Thierry-Chef I, Kesminiene A. Risk of cancer from occupational exposure to ionizing radiation: retrospective cohort study of workers in France, the United Kingdom, and the United States (INWORKS). BMJ 351:h5359; 2015.

Sato K, Takahashi F, Satoh D, Endo A. Development of adult Japanese voxel phantoms and their application to evaluation of radiation exposure doses. Tokaimura: Japan Atomic Energy Agency; JAEA-Data/Code 2010-009; 2010.

Sato K, Takahashi F, Satoh D, Endo A. Construction of average adult Japanese voxel phantoms for dose assessment. Tokaimura: Japan Atomic Energy Agency; JAEA-Data/Code 2011-013; 2011.

Sato K, Takahashi F. The contemporary JAEA Japanese voxel phantoms. Radiat Protect Dosim 149:43–48; 2012.

Sato K, Takahashi F. Construction of adult Japanese voxel phantoms with various body sizes and their applications to evaluation of organ doses due to external photon irradiation (in Japanese). Jpn J Health Phys 52:247–258; 2017.

Sato T, Iwamoto Y, Hashimoto S, Ogawa T, Furuta T, Abe S, Kai T, Tsai P, Matsuda N, Iwase H, Shigyo N, Sihver L, Niita K. Features of particle and heavy ion transport code system (PHITS) version 3.02. J Nucl Sci Technol 55:684–690; 2018.

Thierry-Chef I, Pernicka F, Marshall M, Cardis E, Andreo P. Study of a selection of 10 historical types of dosemeter: variation of the response to *Hp*(10) with photon energy and geometry of exposure. Radiat Protect Dosim 102:101–113; 2002.

Thierry-Chef I, Marshall M, Fix JJ, Bermann F, Gilbert ES, Hacker C, Heinmiller B, Murray W, Pearce MS, Utterback D, Bernar K, Deboodt P, Eklof M, Griciene B, Holan K, Hyvonen H, Kerekes A, Lee M-C, Moser M, Pernicka F, Cardis E. The 15-country collaborative study of cancer risk among radiation workers in the nuclear industry: study of errors in dosimetry. Radiat Res 167:380–395; 2007.

Thierry-Chef I, Richardson DB, Daniels RD, Gillies M, Hamra GB, Haylock R, Kesminiene A, Laurier D, Leuraud K, Moissonnier M, O'Hagan J, Schubauer-Berigan MK, Cardis E, on behalf of the INWORKS consortium. Dose estimation for a study of nuclear workers in France, the United Kingdom and the United States of America: methods for the international nuclear workers study (INWORKS). Radiat Res 183:632–642; 2015.

Tsujimura N, Yamazaki T, Takada C. Present status and practical issues on dosimetry for the lens of the eye at JAEA MOX fuel facilities. J Nucl Sci Technol 58:40–44; 2021.

Vrijheid M, Cardis E, Blettner M, Gilbert E, Hakama M, Hill C, Howe G, Kaldor J, Muirhead CR, Schubauer-Berigan M, Yoshimura T, Ahn Y-O, Ashmore P, Auvinen A, Bae J-M, Engels H, Gulis G, Habib RR, Hosoda Y, Kurtinaitis J, Malker H, Moser M, Rodriguez-Artalejo F, Rogel A, Tardy H, Telle-Lamberton M, Turai I, Usel M, Veress K. The 15-Country collaborative study of cancer risk among radiation workers in the nuclear industry: design epidemiological methods and descriptive results. Radiat Res 167:361–379; 2007.

Yamazaki T, Takada C, Tsujimura N, Okada K. Present status and issues of dosimetry for lens of the eye at the MOX-fuel plant (in Japanese). Jpn J Health Phy 52:167–170; 2017.

∎∎

APPENDIX: PROPERTIES OF LOGNORMAL DISTRIBUTION

When the random variable X follows a lognormal distribution, that is, $\ln(X)$ follows a normal distribution with the mean being μ and the standard deviation being σ, i.e. $\ln(X) \sim N(\mu, \sigma^2)$, the mean and median of X can be expressed as follows:

$$\text{Mean} : E(X) = \exp\left(\mu + \sigma^2/2\right),$$

$$\text{Median} : \text{Med}(X) = \exp(\mu).$$

When the independent random variables X and Y follow a lognormal distribution, i.e. $\ln(X) \sim N(\mu_X, \sigma_X^2)$ and $\ln(Y) \sim N(\mu_Y, \sigma_Y^2)$, the product XY also follows a lognormal distribution because the normal distribution has reproducibility:

$$\ln(XY) = \ln(X) + \ln(Y) \sim N\left(\mu_X + \mu_Y, \sigma_X^2 + \sigma_Y^2\right).$$

■■